GHGT-10

Permeability and injectivity improvement in CO_2 enhanced coalbed methane recovery: Thermal stimulation of the near wellbore region

Amer Syed, Ji-Quan Shi, Sevket Durucan[*]

Department of Earth Science and Engineering, Royal School of Mines, Imperial College London, Prince Consort Road, London SW7 2BP, UK

Abstract

Loss of injectivity in the near wellbore region of coalbeds during CO_2 injection is a limiting factor for its exploitation as potential reservoir for geological storage of CO_2. Current research investigated the potential of thermal stimulation (thermal fracturing through cyclic freezing and thawing) of coal at the wellbore in order to achieve better injectivity during enhanced coalbed methane (CBM) recovery and CO_2 storage. Moisture saturated coal samples were subjected to freezing and thawing cycles to establish the effects of this treatment on coalbed reservoir and elastic properties which can affect CO_2 induced swelling stress and permeability. Volumetric swelling strains were found to be reduced for thermally stimulated coal, resulting in improved permeability. The experimentally measured porosity, elastic modulus and swelling coefficients were then used in an analytical wellbore model to assess the impact of thermal stimulation on near wellbore permeability. Through reservoir simulation studies it was observed that the thermally stimulated zone can potentially improve CO_2 injectivity and enhance methane production.

1. Introduction

Matrix swelling during CO_2 injection in coalbeds results in loss of injectivity due to reduction in near wellbore permeability [1, 2]. Methods that have been suggested to improve the permeability of coalbeds include hydraulic fracturing [3], cavity completion [4, 5] and use of horizontal well technology [6]. It was observed that injection of cold water in warm geothermal wells could result in cracking of the rock matrix, due to thermal contraction of the reservoir rock [7] and effectively increases the porosity and permeability near the injection well. The porosity of the rock is reported to have significant influence on the elastic properties of the matrix [8, 9] and also well-connected pore volumes can improve the permeability within the rock matrix. Recent theoretical studies have found that the swelling of coal is also affected by pore aspect ratio of the coal microstructure and solid (grain) modulus of the coal matrix [10]. Therefore, although conventional well stimulation improves well permeability, it is highly unlikely to impact upon swelling properties of coal in the near wellbore region, which is one of the most important factors affecting well injectivity during CO_2 storage.

Previous research on two different ranks of coal (anthracite and high volatile bituminous B) has shown that temperature has a significant impact on mechanical and elastic properties of coals [11]. The relatively high elastic modulus and brittle high volatile bituminous coal samples have shown an increase in elastic modulus when taken to 0^oC due to stiffening. However, a steady decrease in their bulk elastic modulus was observed as the samples were taken down from ambient temperatures to -25°C, indicating brittle fracturing throughout. The thermal stresses induced during freezing can initiate microcracks or will lead to propagation of existing cracks and eventually lead to increase in void volume and reduction in elastic properties [8, 9].

Following on from these previous studies, current research investigated the effect of cyclic freezing/thawing on elastic properties, permeability and swelling behaviour of the same anthracite (Selar 9ft seam in South Wales, UK) and low rank high volatile bituminous B coal (Schwalbach seam in Saarland, Germany). The main objective of the research was to investigate the

---

[*] Corresponding author. Tel.: +44-20-7594-7354; fax: +44-20-7594-7354.
E-mail address: s.durucan@imperial.ac.uk.

potential of thermal stimulation (thermal fracturing) of coal to achieve better injectivity of CO_2 during enhanced CBM recovery and CO_2 storage. Research also aimed at establishing the effects of thermal fracturing and interaction with CO_2 on the mechanical/elastic properties of coal and its swelling/shrinkage behaviour in order to implement these findings in a wellbore and far field permeability model in order to assess field behaviour. Laboratory experiments were carried out to assess the effect of thermal cycling on matrix swelling strains during CO_2 injection. The results obtained were implemented in an analytical wellbore model and a reservoir simulator to study the impact of thermal stimulation on the permeability and well injectivity.

2. Experimental investigations

Moisture saturated core plugs of 38mm diameter (76mm long) and 50mm diameter (100mm long) were used for porosity, permeability, mechanical and elastic properties testing. Cubic samples (side <25.4mm) were prepared for the swelling strain experiments. The samples were scanned for NMR logs to determine the (a) spin-spin (T_2) relaxation time distribution which is analogous to the pore size distribution of coal [12] and (b) porosity. The samples were then subjected to a temperature of -25°C in a laboratory freezer for 24 hours and subsequently heated to 40°C in a laboratory oven. This marked the completion of one thermal cycle after which the samples were again moisture saturated and the freezing-thawing cycle was repeated.

At the end of three thermal cycles, the 38mm cylindrical samples were subjected to multistage triaxial tests to determine the elastic modulus, Poisson's ratio and mechanical strength in order to assess the effect of thermal cycling on mechanical and elastic properties of coal. The cubic samples were used for matrix swelling tests and the 50mm diameter cylindrical samples for the simultaneous strain and permeability measurements. The matrix swelling experiments on cubic samples are used to determine the Langmuir pressure, Langmuir strain and swelling coefficient to be used for modelling the swelling induced permeability behaviour of thermally stimulated coal. The simultaneous strain permeability measurements provide a direct assessment of the change in coal permeability during CO_2 injection. Detailed description of the experimental setup, procedure and data analysis is described elsewhere [13, 14]. Swelling strain measurements were conducted at constant temperature of 40°C and were pressurised with CO_2 from 0 to 3.5MPa in steps of 0.5MPa. For simultaneous strain-permeability measurements, the experiments were carried out at constant pore pressures of 0.6 MPa and 2.7 MPa with varying effective stresses.

3. Results and discussion

3.1. Effect of thermal cycling on coal properties

It was observed that repeated thermal cycling effects the pore size distribution of the coal. Figure 1a presents the pore size distribution of Selar coals before and at the end of each thermal cycle for three cycles. At the end of the first thermal cycle for the Selar coal sample (Figure 1a) the population of micropores ($T_2<1ms$) was observed to have increased and some of the micropores would have been connected in the process, thus increasing the size of the crack/pore, which is reflected by the rightward movement of the pore size distribution curve. This process of reconnection of pores due to new fractures has been observed at the end of each thermal cycle indicating the progressive fracturing of the coal matrix. Also observed is the increase in the pores of sizes corresponding to meso ($1ms<T_2<100$) and macropores ($100<T_2<1000$) region. Similar observations were made for the pore size distribution of the Schwalbach coal sample.
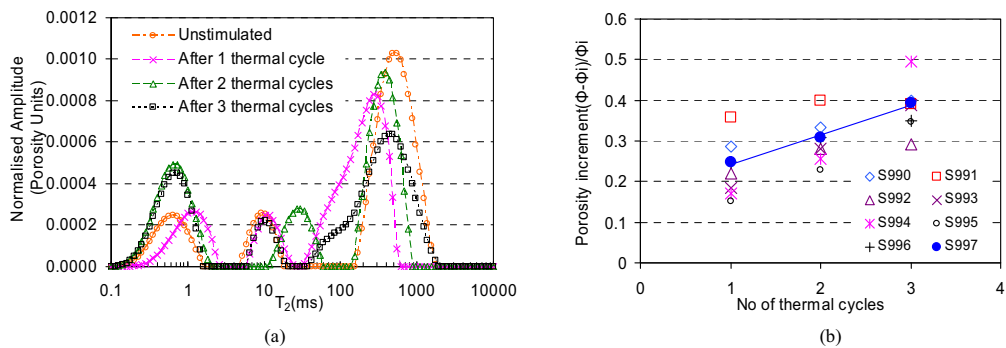

Figure 1. (a) Change in pore size distribution of Selar 9ft (S9 710) coal throughout the thermal cycles (TC-1, 2 and 3 indicate the measurements carried out after first, second and third thermal cycles); (b) The effect of thermal cycling on porosity of Selar 9ft coal.

The total porosity calculated using the pore size distributions have shown progressive increment with the number of thermal cycles resulting in an increase in fracture density. The increase in porosity of different samples with an increase in the number of thermal cycles is presented in Figure 1b.

The analysis of multi stage triaxial test results have shown that the elastic modulus of thermally cycled Selar coal was reduced by 27%, the axial compressive strength by 65% and the tensile strength by 91% compared to non-thermally cycled coals (Table 1). The loss of tensile strength strengthens the argument that thermal cycling induces brittleness in coal. Compared to the high rank Selar coal, the change in elastic properties of low rank Schwalbach coal have been marginal.

Table 1. Comparison of elastic properties for thermally stimulated coal with that of unstimulated coals.

	Schwalbach		Selar	
	Unstimulated	**Thermally stimulated**	**Unstimulated**	**Thermally stimulated**
Elastic Modulus (matrix), GPa	3.30	3.2	2.14	1.56
Poisson's ratio	0.26	0.3	0.4	0.43

3.2 Effect of thermal cycling on matrix swelling strains

Figure 2a shows the linear matrix swelling strains measured on Selar 9ft (S9) cubic samples, which have been taken through the same thermal cycles described earlier in section 2. The same figure compares the swelling strains obtained for these samples with the swelling strains determined for non thermally cycled coal samples (though different cube samples). Good consistency between the two strain gauges (A and B), and among the samples for the coals is noted. The swelling strains for thermally stimulated coals are observed to be relatively low compared with that of the unstimulated coals.

In order to explain the reduction in matrix swelling strains for thermally cycled coal samples, the measured swelling strains were analysed using a theoretical micromechanical model for coal matrix swelling that is based on the thermodynamic interactions relating the changes in surface energy of the coal during adsorption of gases to the elastic response of the coal [10]. Mathematically, the equilibrium matrix strain in coal due to adsorption of gas is given as

$$\varepsilon = RTL \ln(1 + Bp)\frac{\rho_s}{E_s} f(x, v_s) - \frac{P}{E_s}(1 - 2v_s) \qquad (1)$$

where R is the universal gas constant, T is temperature, L and B are Langmuir Parameters, P is the pore pressure, E_s and v_s are the modulus of elasticity and Poisson's ratio, and the parameter $f(x, v_s)$ is defined as

$$f(x, v_s) = \frac{[2(1 - v_s) - (1 + v_s)cx][3 - 5v_s - 4(1 - 2v_s)cx]}{(3 - 5v_s)(2 - 3cx)} \qquad (2)$$

and the microstructural porosity is defined as

$$\phi = 1 - 3\pi x^2(1 - cx) \qquad (3)$$

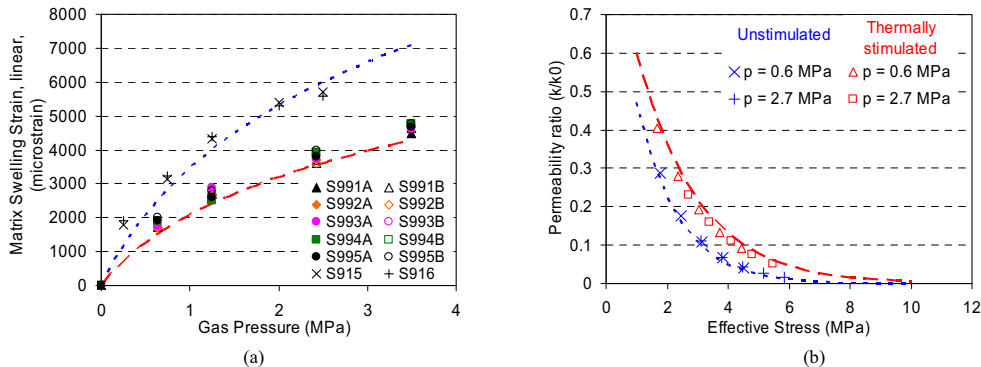where ϕ is the porosity and $c = 1.2$.

Figure 2. (a) The effect of thermal cycles on swelling strains of Selar 9ft (S9) coals. The strains measured parallel to the bedding plane are shown in filled symbols and those measured perpendicular to the bedding plane are shown with open symbols. Samples tested without thermal cycling are shown using symbols '+' and 'x'; (b) The effect of thermal fracturing on permeability of coal Selar 9ft coal. The symbols '+' and 'x' indicate the measurements carried out before thermal cycling.

The model predictions for swelling strains of coals with and without thermal stimulation are plotted as dotted trend lines in Figure 2a above. The model results are matched with the experimental results by varying the parameter x and relating the dimensions of micromechanical skeleton to its porosity [15]. The porosity calculated is also independently verified by the tests conducted in the laboratory. From the NMR measurements the change in porosity due to thermal fracturing of Selar coals was observed to be in the range of 20 to 50%. The model match suggested a change in porosity of 20%, which represents the lower range of that observed from the experimental data. The parameters used in the modelling work are presented in Table 2.

3.3. Sorption induced permeability changes during CO_2 injection

Permeability of coal is highly stress dependent [16]. Sorption induced changes in stresses depend on the elastic response of coal, and any change in coal elastic properties are likely to alter this behaviour. Hence, the elastic response of coal through the reduction in matrix swelling strains (Figure 2a) is reflected as an increase of permeability for thermally cycled coals (Figure 2b).

Table 2. Parameters used in the theoretical model to match experimental data.

	Schwalbach		Selar	
	Unstimulated	Thermally stimulated	Unstimulated	Thermally stimulated
Elastic Modulus (matrix), GPa	3.30	3.20	2.14	1.56
Poisson's ratio	0.26	0.30	0.40	0.43
x	0.55	0.549	0.541	0.525
Porosity (%) (Calculated from equation 3)	3.050	3.060	3.233	3.884

4. Effect of thermal stimulation on CO_2 injectivity of coalbed methane wells

Experimental work carried out has indicated that the coal properties, namely the elastic modulus, porosity, permeability and matrix swelling coefficient were altered by the thermal treatment. It is expected that thermal stimulation through cyclic freezing and thawing of a coalbed methane wellbore would create a stimulated zone with altered reservoir and rock properties (Figure 3), the extent of which will depend on the area subjected to the temperature gradient. This section presents the findings of analytical and numerical simulations carried out in order to estimate the effect of such thermally stimulated zone on reservoir performance. The data used in the modelling studies is given in Table 3.

Table 3. Fluid and reservoir properties used in modelling near wellbore effects of thermal stimulation.

Fluid Properties	N_2 (at 12 MPa and -25 ^{0}C)	CO_2 (at 12 MPa and 40 ^{0}C)
Density (kg/m^3)	170.04	717.76
Viscosity (x10^{-5} Pa-s)	1.9037	5.8528
Heat Capacity of the fluid (J/kg K)	1355.0	3427.6
Thermal conductivity (W/mK)	0.03099	0.078042

Elastic and Swelling Properties	Unstimulated	Thermally Stimulated
Elastic Modulus (GPa)	2.14	1.56
Poisson's Ratio (dimensionless)	0.40	0.43
Langmuir Pressure (MPa) – CO_2	0.77	0.77
Langmuir strain (dimensionless) - CO_2	0.020	0.018

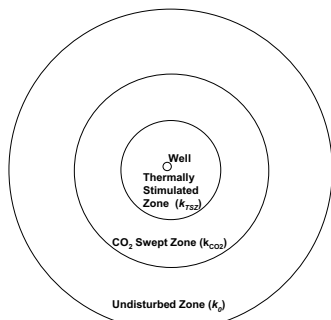| Coalbed Reservoir Properties			
Depth (m)	1200	Radius of the wellbore (m)	0.1524
Porosity (%)	1	Permeability (mD)	1
Heat capacity (J/Kg K)	1089	Coefficient of Linear Expansion (10^{-6}/^{0}C)	16

Figure 3. Schematic representation of a uniform thermally stimulated zone around the injection wellbore.
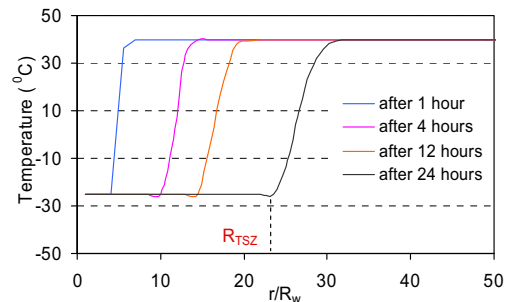

Figure 4. Predicted near wellbore temperature over 24 hours of cold nitrogen injection.

4.1. Extent of the thermal stimulation zone

During injection of cold fluid, heat transfer is primary by convection and would depend on the thermal properties of the injected fluid and coal. The convection dominated heat transfer results in a sharp temperature front, the (relative) speed of which is primarily controlled by the product of density and heat capacity of the fluid [17]. The temperature distribution around the injection well can be calculated based on energy balance considerations [18] and can be given as

$$T = T_r + (T_w - T_r)e^{-w}\int_0^{r'} e^{-z}I_0[2\sqrt{zw}]ds \qquad (4)$$

where T_r and T_w are the temperature of the reservoir and the wellbore respectively. Parameters r', z and w are defined as

$$r' = \sqrt{2v_w tR_w + R_w^2} - r \qquad (5\ a)$$

$$z = \frac{1}{2}\frac{H\gamma}{\phi v_w \rho_f c_f R_w}\left(r^2 - R_w^2\right)$$

(5 b)

$$w = \frac{H\gamma}{(1-\phi)v_w \rho_s c_s}\left(v_w t - \frac{s^2}{2R_w} + \frac{R_w}{2}\right)$$

(5c)

where R_w is the radius of the wellbore, r and t are spatial and temporal variables, v_w is the constant fluid velocity at the borehole wall, H is the heat transfer coefficient, γ is specific surface area of the rock, ϕ is porosity, ρ_f and ρ_s are the densities of the fluid and rock, c_f and c_s are the heat capacities of the fluid and rock.

In this study, the injection fluid temperature was assumed to be -25°C in order to be compatible with the laboratory experiments. The thermally stimulated zone (TSZ) is defined as an area (with a radius R_{TSZ}) around the injection wellbore where the temperature of the formation is cooled down to -25°C. The temperature profile created around the injection well during cold nitrogen injection into the reservoir (40°C) is calculated using equations 5a, 5b and 5c. As illustrated in Figure 4, the thermally stimulated zone extends into the reservoir with time. However the thermal properties (density, heat capacity and thermal diffusivity) of cold nitrogen and coal will be the limiting factors for the maximum extent of thermally stimulated zone that can be achieved. For the case illustrated here, the radius of the thermally stimulated zone reaches 5 times the injection well radius in the in the first hour of cold injection. Further three hours are required for the stimulated zone radius to reach $10R_w$, and a full day to extend to $25R_w$. In the study described here, $R_{TSZ}/R_w = 25$ is taken as the extent of thermally stimulated zone for further analysis.

4.2. Sorption induced permeability in the near wellbore region

Experimental observations have shown that the properties of coal in the thermally stimulated zone are likely to be altered by the process of thermal cycling. In particular, cyclic freezing and thawing would result in reduced elastic modulus and swelling strain. The combined effect of this change on permeability response to CO_2 injection can be evaluated taking in to account the effects of CO_2 adsorption/swelling, as well as coal properties, on the formation stresses in the near wellbore region. An analytical model to calculate the sorption induced stresses in coalbeds during primary and enhanced methane recovery is proposed here. The general equation for radial stress is given as

$$\sigma_r(r) = 2(\lambda+2G)A_g - 2G\frac{B_g}{r^2} - \frac{\lambda+G}{\lambda+2G}\alpha p - \frac{\lambda+G}{\lambda+2G}\left(\lambda+\frac{2}{3}G\right)\alpha_s v_L \frac{p}{p+p_L} - \frac{G}{\lambda+2G}\frac{b}{2} - \frac{\lambda+G}{\lambda+2G}\left(\lambda+\frac{2}{3}G\right)\frac{\alpha_s v_L p_L}{b}2\exp\left[-\frac{2(a+p_L)}{b}\right]Ei\left[\frac{2(p+p_L)}{b}\right]\frac{1}{r^2}$$
$$+\frac{G}{\lambda+2G}\left(\lambda+\frac{2}{3}G\right)\alpha_s v_L \frac{p_L}{p+p_L} + \alpha(p-p_0) + \left(\lambda+\frac{2}{3}G\right)\alpha_s v_L \frac{p}{p+p_L} - \left(\lambda+\frac{2}{3}G\right)\alpha_s v_L \frac{p_0}{p_0+p_L}$$

(6)

where G and λ are the Lamé parameters, p_L and v_L are Langmuir pressure and volume respectively, α_s is the swelling coefficient, $Ei(x)$ is the exponential integral, A and B are constants to be determined by solving for appropriate boundary conditions.
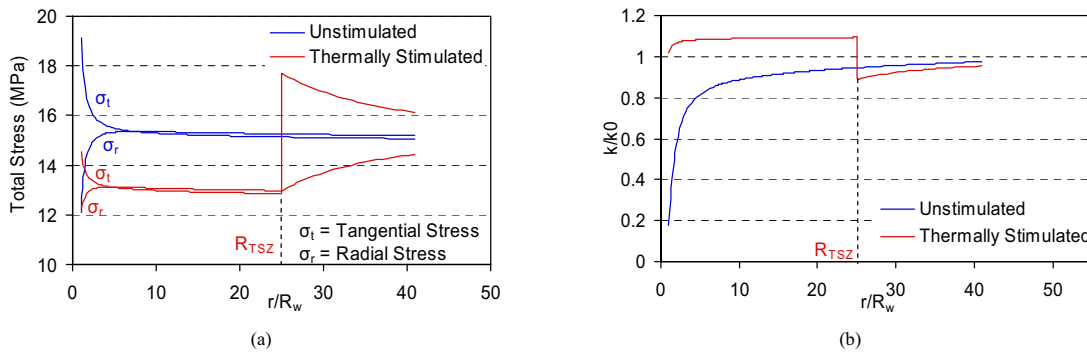

Figure 5. Impact of thermally stimulated zone on (a) near wellbore stresses and (b) radial permeability of coal in the near wellbore region.

Although transition from the thermally stimulated zone to the undisturbed zone may, in reality, be gradual, here it was assumed that the elastic and swelling properties of coal would change at the boundary of the thermally stimulated zone ($r = R_{TSZ} = 25R_w$). The sorption induced stresses in the near wellbore region were then calculated for isothermal injection at a constant injection pressure of 12 MPa, using Equation 6 and the properties listed in Table 3. The radial and tangential stress profiles calculated indicate that stresses in the thermally stimulated zone are lower than that experienced in an unstimulated wellbore due to the reduced elastic and swelling properties (Figure 5a). The sharp increase in the tangential stresses at the boundary of thermally stimulated zone is due to the assumption that the transition between the thermally stimulated and unstimulated zones is abrupt which, in reality, would be much smoother. For fluids flowing into and out of the wellbore, the tangential stress acting in

the direction normal to the flow would be important in determining the stress dependent permeability. Permeability was calculated using the exponential relationship $k=k_0\exp(-3c_f(\Delta\sigma_t))$ where $\Delta\sigma_t$ is the change in tangential stress due to CO_2 injection and matrix swelling (Figure 5b). For the current test case, the permeability is improved in the thermally stimulated zone, resulting from the altered swelling and elastic properties.

4.3. Impact of thermal stimulation on CO_2 injectivity

In reservoir simulations, changes in formation permeability in the immediate vicinity of a wellbore, due either to stimulation or mud damage, are commonly represented using a skin factor S. In Equation 7, R_{skin} is the radius of the zone of the zone which has a different permeability (k_{skin}) than the formation permeability (k_0)

$$S=\left(\frac{k_0}{k_{skin}}-1\right)\ln\left(\frac{R_{skin}}{R_w}\right) \tag{7}$$

For reservoir simulation of CO_2 into thermally stimulated wells, equation 7 may be written as

$$S=\left(\frac{k_{CO2}}{k_{TSZ}}-1\right)\ln\left(\frac{R_{TSZ}}{R_w}\right) \tag{8}$$

where k_{CO2} and k_{TSZ} (Figure 3) are respectively the CO_2 affected permeability within and outside the thermally stimulated zone during CO_2 injection. Here it is assumed that the injected CO_2 has migrated outside the thermal stimulation zone and the permeability of the CO_2 swept zone has largely stabilised. The skin factor calculated using Equation 7 was found to be in the range -0.5 to -3.0 for R_{TSZ}/R_{CO2}=5 and R_{TSZ}/R_{CO2}=30. For the analysis carried out in section 4.2, the average permeability ratio for R_{TSZ}/R_{CO2}=25 was 1.255. The equivalent skin factor for this value is calculated as -0.65.

For illustration purposes, numerical simulations were carried out using a 915m x 915m (~200 acres) coalbed methane reservoir. A total seam thickness of 9m was assumed and simulations were conducted using a 5 –spot well pattern with 50m x 50m grid block size in METSIM2, Imperial College's in-house CBM/ECB simulator. During reservoir simulations, the centre well was turned to a CO_2 injection well in the second year. To represent the impact of thermal stimulation on CO_2 injectivity, a skin factor of -0.65 was used. The simulated cumulative CO_2 injection and methane production over a 10 –year period for a thermally stimulated well (S = -0.65) is compared with that of an unstimulated well (S=0) in Figure 6. It can be seen that the cumulative CO_2 injection is enhanced by approximately 11% for the thermally stimulated case. A marginal improvement in methane production is also observed.
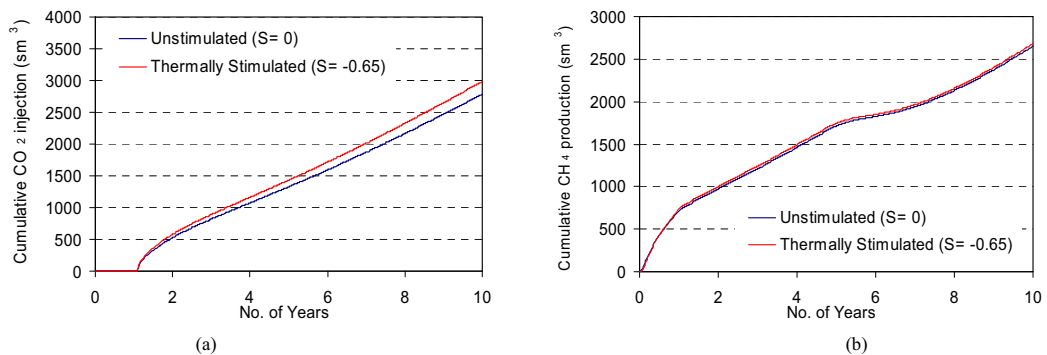

Figure 6. Simulated cumulative (a) CO_2 injection and (b) methane production volumes for the thermally stimulated and unstimulated wells.

5. Conclusions

Research presented in this paper investigated the potential of thermal stimulation/fracturing of coal at the wellbore in order to achieve better injectivity during enhanced coalbed methane (CBM) recovery and CO_2 storage. Moisture saturated coal samples were subjected to freezing and thawing cycles to establish the effects of this treatment on coalbed reservoir and elastic properties which can affect CO_2 induced swelling stress and permeability. Matrix swelling strains due to CO_2 injection in thermally stimulated coal was observed to be lower than that of unstimulated coals. Comparison with the results of a theoretical sorption and matrix swelling model indicated that the change in porosity, pore aspect ratio and elastic properties of coal contributes to the reduction in matrix swelling strains in thermally stimulated coals. The experimentally measured porosity, elastic modulus and swelling coefficients were used in an analytical wellbore model to assess the impact of thermal stimulation on near wellbore permeability. The potential improvement in CO_2 injectivity and enhance coalbed methane production was investigated through reservoir simulation.

References

[1] Reeves, S., Taillefert, A., Pekot, L. and Clarkson, C., 2003. The Allison Unit CO_2 – ECBM pilot: A reservoir modelling study, DOE Topical Report.

[2] Shi, J-Q., Durucan, S. and Fujioka, M., 2008. A reservoir simulation study of CO_2 injection and N_2 flooding at the Ishkari coalfield CO_2 storage pilot project, Japan. Int. J. Greenhouse Gas Control. 2, 47-57.

[3] Colmenares, L.B. and Zoback, M.D., 2007. Hydraulic fracturing and wellbore completion of coalbed methance wells in Powder River Basin, Wyoming; Implications for water and gas production. AAPG Bull. 91(1), 51-67.

[4] Palmer, I.D., Mavor, M.J., Spitler, J.L., Seidle, J.P. and Volz, R.F., 1993. Openhole cavity completions in coalbed methane wells in the San Juan Basin. J. Petrol. Technol. 45(11), 1072-1080.

[5] Sinka, I. C., 1998. An investigation into rock and reservoir properties of coal with special reference to stimulated coalbed methane well performance. PhD Thesis, Imperial College London.

[6] Ertekin, T., Sung, W. and Schwerer, F.C., 1998. Production performance analysis of horizontal drainage wells for degasification of coal seams. J. Petrol. Technol. 625-632.

[7] Clifford, P. J., Berry, P.J. and Hongren, Gu, 1991. Modelling the vertical confinement of injection well thermal fractures. SPE Production Engineering . 6(4), 377-383.

[8] Walsh, J.B., 1965a. The effect of cracks in the compressibility of rock. J. Geophys. Res. 70(2), 381-389.

[9] Walsh, J.B., 1965b. The effect of cracks in rocks on Poisson's ratio. J. Geophys. Res. 70(20), 5249-5257.

[10] Pan, Z. and Connell L.D., 2007. A theoretical model for gas adsorption-induced coal swelling. Int. J. Coal Geol. 69(4), 243-252.

[11] Durucan, S., Shi, J-Q. and Grattoni, C.G., 2005. Thermal stimulation in coal: An investigation into the potential permeability effects of cold CO_2 injection for enhanced coalbed methane recovery. A Technical Report submitted to Shell International Exploration and Production.

[12] Xu, X. and Davis, L.A., 1999. The relation of poresize to NMR T_2 diffusional relaxation in porous media. SPE 56800. Presented at the Annual Technical Conference and Exhibition, Houston, USA.

[13] Ahsan, M., 2006. Gas flow and retention characteristics of coal seams for enhanced coalbed methane recovery and CO_2 storage. PhD Thesis, Imperial College London.

[14] Durucan, S., Ahsan, M. and Shi, J.Q., 2009. Matrix shrinkage and swelling characteristics of European coals. Energy Procedia. 1, 3055-3062.

[15] Scherer, G.W., 1986. Dilatation of porous glass. J. Am. Ceram. Soc. 69 (6), 473-480.

[16] Durucan, S. and Edwards, J., 1986 Effects of stress and fracturing on permeability of coals. Min. Sci. Tech. 3(3), 205-216.

[17] Fjær, E., Holt, R.M., Horsrud, P., Raaen, A.M. and Risnes, R., 2008. Petroleum Related Rock Mechanics, 2nd ed., Elsevier, Amsterdam.

[18] Hojka, K., Dusseault, A.D. and Bogobwicz, 1993. Analytical solutions for transient thermoelastic stress fields around a borehole during fluid injection in permeable media. J. Can. Petrol. Tech. 32(4), 49-57.